



Western Washington University
Western CEDAR

WWU Honors Program Senior Projects

WWU Graduate and Undergraduate Scholarship

Spring 2003

Increasing Expression Yields of Circularly-Permuted Myoglobins

Casey Kulla

Western Washington University

Follow this and additional works at: https://cedar.wwu.edu/wwu_honors

 Part of the [Chemistry Commons](#)

Recommended Citation

Kulla, Casey, "Increasing Expression Yields of Circularly-Permuted Myoglobins" (2003). *WWU Honors Program Senior Projects*. 248.

https://cedar.wwu.edu/wwu_honors/248

This Project is brought to you for free and open access by the WWU Graduate and Undergraduate Scholarship at Western CEDAR. It has been accepted for inclusion in WWU Honors Program Senior Projects by an authorized administrator of Western CEDAR. For more information, please contact westerncedar@wwu.edu.

Increasing Expression Yields of Circularly-Permuted Myoglobins

**by
Casey Kulla**

**A Thesis Presented
To the Faculty of
The Chemistry Department of
Western Washington University**

**Submitted in Partial Fulfillment
Of the Requirements for the
Bachelor's Degree with
Honors in Biochemistry**

**Supervised by Professor Spencer Anthony-Cahill
Department of Chemistry
The College of Arts and Sciences
Western Washington University
June 2003**

HONORS THESIS

In presenting this Honors paper in partial requirements for a bachelor's degree at Western Washington University, I agree that the Library shall make its copies freely available for inspection. I further agree that extensive copying of this thesis is allowable only for scholarly purposes. It is understood that any publication of this thesis for commercial purposes or for financial gain shall not be allowed without my written permission.


Signature  Casey Kulla
Date 6-12-03

TABLE OF CONTENTS

	PAGE
Abstract	ii
Acknowledgements	iii
List of Figures and Tables	v
Background	1
Introduction	2
HGL16 topological mutation	4
MBP fusion system	5
Direct Expression of ApoMb	5
H64F stabilizing mutation	6
Materials and Methods	7
Recombinant DNA	7
Protein Purification	12
Protein Characterization	14
Results	17
MBP-HGL16	17
Direct Expression of ApoMb	20
H64F-HGL16	24
Discussion	30
MBP-HGL16	30
Direct Expression of ApoMb	31
H64F-HGL16	33
Conclusions	35
References	37

Abstract

The permuted myoglobin HGL16 is known to be structurally and functionally similar to the wild-type (wt) sperm whale myoglobin (swMb) yet is less stable to chemical denaturation by 5.2 kcal/mole. Given published reports that stabilities of myoglobin mutants are correlated to expression yields and our own confirmation of this correlation, we are eager to increase expression yields of our destabilized permutants to facilitate protein characterization. One method, fusing HGL16 to Maltose-Binding Protein (MBP), increases yields but appears to destabilize the fused HGL16. Another method for increasing yields, overexpressing protein in the form of inclusion bodies, is particularly useful as it yields apo-myoglobin (apoMb), necessary for investigating true two-state unfolding and the apoMb pH 4.2 intermediate. Urea denaturation studies show our methods of purification are valid, but pH denaturations of our directly expressed, purified apo wt myoglobin remain inconclusive. Further, mutating the distal histidine to phenylalanine (H64F) has been shown to increase the stability of wt swMb, at the cost of impaired function. Introducing an H64F mutation into the HGL16 permutein results in soluble protein with similar expression yields to HGL16 but with a shifted heme absorbance. Preliminary characterization studies yield a reproducible and non-cooperative denaturation curve for holo-H64F-HGL16.

ACKNOWLEDGEMENTS

Many thanks to Spencer Anthony-Cahill, Alexei Lissounov, and the other members of Team Spencer for guidance, encouragement, and the occasional whip.

Many thanks to Lisa Gentile for the gift of the pMAL plasmid, genenase, and PMSF.

Many thanks to H. Jane Dyson for the gift of the pET17b plasmid and the inclusion body protocol.

Many thanks to Katie Kulla for patience, encouragement, and staying up late.

Many thanks to James Vyvyan for telling me to stay away from Biology and Medicine.

Many thanks to Carolyn Bertozzi for claiming I am more enthusiastic than she.

Many thanks to Carol Trent for telling me she'd write a letter of reference only if it was for graduate school—not medical school letters for me. I didn't believe you.

(I sense a conspiracy.)

Many thanks to the Chemistry faculty and staff for giving me lots of money, recognition, support and teaching me about molecules and life.

Finally, many thanks to the Western Plumbing Shop gentlemen—you practically forced me back into school. Thank you.

You've all taught me. A priceless gift. I hope I can repay the favor.

LIST OF FIGURES AND TABLES

	PAGE
Figure 1: Generic circular permutation diagram	3
Figure 2: A-H helices in swMb and HGL16 diagram	4
Figure 3: SDS-PAGE of MBP-HGL16	18
Figure 4: SDS-PAGE of MBP-HGL16 cleavage reactions	19
Figure 5: Urea denaturation of MBP-HGL16 compared to HGL16	20
Figure 6: SDS-PAGE of apoMb overexpression	21
Figure 7: SDS-PAGE of apoMb purification	21
Figure 8: CD spectrum of purified apoMb	22
Figure 9: Reverse-phase HPLC of apoMb and holoMb	23
Figure 10: Urea and pH denaturations of apoMb	24
Figure 11: SEC trace for purification of H64F-HGL16	25
Figure 12: SDS-PAGE of purified H64F-HGL16	26
Figure 13: UV-Vis absorbance trace of H64F-HGL16	26
Figure 14: Urea denaturation of H64F-HGL16, UV-Vis	27
Figure 15: CD spectra of H64F-HGL16 and HGL16	28
Figure 16: Urea denaturation of H64F-HGL16 compared to HGL16, CD	29
Figure 17: Overlaid CD and UV-Vis data for H64F-HGL16	29
Figure 18: Cartoon of MBP-HGL16 fusion protein	30
Table 1: MBP-HGL16 primers	10
Table 2: H64F-HGL16 mutagenic primers	11
Table 3: HGL16 pET17b primers	11
Table 4: Yields of HGL16 and MBP-HGL16	17
Table 5: Yields of apoMb from direct expression vs. heme extraction	21
Table 6: Yields of HGL16 and H64F-HGL16	26

Background:

Sperm whale myoglobin, our research group's model protein, functions as an oxygen-binding protein. While similar to the four subunits of hemoglobin, myoglobin binds oxygen more tightly than hemoglobin; myoglobin is found in large concentrations in muscle tissue, where oxygen is needed for muscle function. As the partial pressure of oxygen falls during aerobic exercise, myoglobin begins to release its bound oxygen, modulating the decrease.

As a model system, myoglobin is excellent. It is small (153 amino acids), like other globin proteins. When the heme group—which binds oxygen—is removed, myoglobin shows prototypical two-state unfolding, making calculations of free energy simple. As an all-alpha helical protein, myoglobin is easily monitored by circular dichroism spectroscopy (CD), providing a clear, native-protein method for monitoring changes in secondary structure. On account of the heme group, myoglobin is red in color, and can be qualitatively visualized in a heterogeneous protein pool or quantitatively by the heme's characteristic, native-protein absorbance at 418 nm (the Soret absorbance).

Myoglobin was the first protein to have its three-dimensional structure solved, in 1961 by John Kendrew and associates; since then, many mutants of myoglobin, with many states of the heme (cyano, met, aquo, etc.), have been characterized. Typically, a researcher would avoid such a canonical protein in the search for novel protein structures. However, for our work, *circular permutation* of sperm whale myoglobin (see introduction for specifics), the extensive characterization of myoglobin is our foundation. We want to learn what happens when a large region of the primary structure of

myoglobin is moved around in the protein—for this, we must compare our novel forms to the native structure.

Introduction:

Methods for increasing expression yields will be essential in the development of engineered proteins as drug therapeutics and diagnostics, as well as industrial process catalysts. It is likely that increasing yields will not be simply a matter of increasing the stability of the folded protein—due to the need to balance protein stability and function. Chemical and thermal stability are not always correlated with desired protein activity (1). To increase yields, protein chemists must understand the processes underlying stability, solubility, and folding pathways of proteins.

The function, stability, folding pathway and denaturant-stabilized intermediates of sperm whale myoglobin (swMb) have been extensively characterized (2, 4, 5, 11-17). Apomyoglobins of swMb—apo is the protein without the heme ligand, while holomyoglobin contains the heme—have been studied most closely due to the more truly two-state unfolding and folding of apoMb compared to holoMb (2, 11-14, 16). Point mutations may give clues to the local environments of amino acid residues in folded swMb, but more information is needed to address larger issues such as how an entire region is structured in folding intermediates such as the molten globule (MG). The MG is a pH-stabilized intermediate in apoMb believed to be on the folding pathway from unfolded to folded, native myoglobin—the molten globule contains much of the secondary structure of the native state but few of the specific tertiary contacts found in the native structure of apoMb (2).

We want to probe the question of how, during folding, an entire region of a protein may undergo structural change. A topological mutation, such as physically linking the A and H helices of swMb, can be used to answer this question of what may be necessary for globin protein folding. Circular permutation is one method of changing topology in a protein. This method involves linking the N- and C-termini of the protein

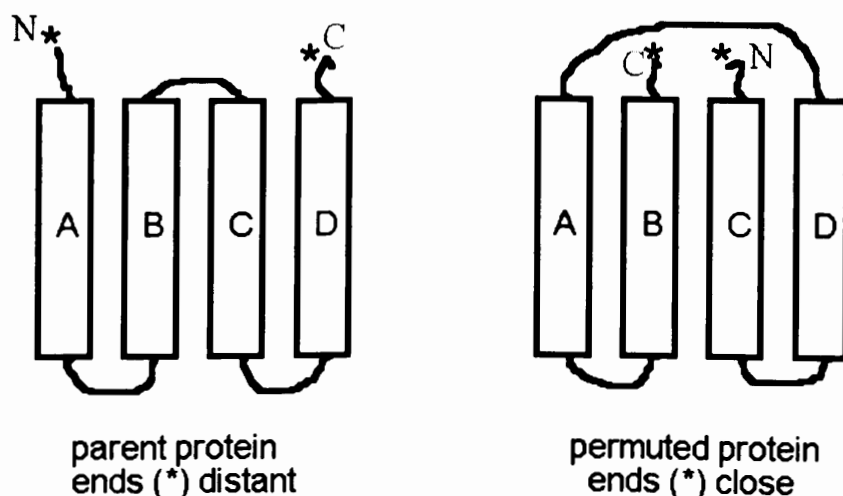


Figure 1. In circular permutation, the original N- and C-termini are connected by a linker and new N- and C-termini are created within the protein. This changes the arrangement of the secondary structural elements, which are shown as rectangles in this diagram.

with an unstructured peptide linker and creating new N- and C-termini between any two amino acids in the protein (Figure 1). Circularly-permuted proteins are known as circular permuteins. Circular permutation is useful for probing how primary sequence and functional tertiary structure are related, and Iwakura *et al.* 2000 have shown that new termini can be inserted nearly anywhere in a model protein by systematically permuting each residue—creating as many permuteins as there are residues in the protein (3).

With eight alpha helices, A-H, swMb is a good candidate for circular permutation, as one helix at a time could be moved to the N-terminus of the protein. A

circular permutein of swMb (Figure 2), where the native N- and C-termini are spanned by a 16 residue linker (SGGG)₄, and new termini are created in the loop between the G and H helices (Pro 120 is the new C-terminus and Gly 121 is the new N-terminus), has been reported recently (4). This new circular permutein, “HGL16,” was shown to be similar in ligand binding and folded structure to wt swMb, though thermodynamically destabilized by 5.2 kcal/mol.

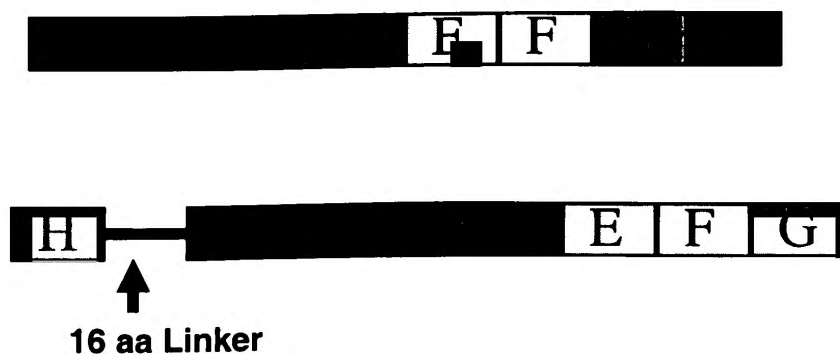


Figure 2: Schematic drawing of the eight alpha helices in swMb, with the HGL16 permutein below.

The gene encoding swMb has been optimized for expression in bacteria (15), but low expression yields plague the HGL16 permutein, corroborating an observation that destabilizing mutants of swMb show decreased yields relative to wt (5). Further characterization of HGL16, including NMR structure solution (which requires up to 30 mg of protein), stopped-flow experiments, and apoprotein folding experiments, necessitates increasing the expression yield of recombinant protein. Additionally, studies of HGL16 require that current researchers purify liter upon liter of cell culture before any characterization can begin, greatly slowing the pace of experimentation.

We explored three methods for increased expression of HGL16 permuted myoglobins: (1) a fusion protein system involving Maltose-Binding Protein (MBP), (2)

apo-protein expression using a modified inclusion body protocol, and (3) a stabilizing point mutation, H64F. Together, these methods probe issues of solubility, stability, and partnered promotion: is there more than increased stability to increased expression of engineered proteins?

Protein fusion systems have been used extensively to increase expression, stability, solubility, and ease purification of target proteins. It is postulated that a highly-expressing protein, when fused to a target protein, promotes expression of the target by stabilizing it and slowing *in vivo* proteolytic degradation. MBP is a popular fusion partner (6-10), used, for example, in high throughput proteomics for expressing human proteins of unknown structure and function. Ideally, the target protein is cleaved from MBP in the purification process, allowing for characterization solely of the target. We explore whether fusing MBP to HGL16 increases expression of HGL16; we do this by fusing them, performing expression studies and optimizing cleavage of the fusion protein. We also looked at the effect of MBP fusion on the stability of HGL16 by denaturing the fusion protein.

The high-level overexpression of apoMb in *E. coli* leads to aggregation of the protein into insoluble “inclusion bodies.” Continuing this overexpression can make target protein comprise up to 50% of total cellular protein. As bacteria do not make heme at the rate of apomyoglobin production, the inclusion bodies contain nearly pure apo-protein; as well, aggregates do not have a heme binding pocket. This is crucial for our lab, given the already low yields of holo-HGL16. Extracting the heme requires unfolding the protein—upon refolding, 80% of the starting HGL16 is lost through aggregation. Apomyoglobin is desirable as mentioned above because it represents more closely a true two-state

system; most swMb studies of folding are therefore performed with apoMb (e.g., the pH 4.2 apoMb intermediate has been extensively characterized: 11-14). As HGL16 must be compared to wt, the increased and direct production of apo-HGL16 is crucial to our understanding of how topological mutations affect folding pathways.

Stabilizing point mutations in wt swMb have been reported (13). Mutating the distal histidine (H64, E helix) to phenylalanine causes the protein to gain stability through the hydrophobic effect and the reduction in solvated surface area. Some loss of function is seen with this mutation, as H64 coordinates the binding of oxygen and discriminates against carbon monoxide (16); however, there is an observed increase in stability of unfolding, $\Delta\Delta G_{H20}^{\circ} = + 2.8$ kcal/mol for apo-H64F vs. wt swMb, with a change in C_m of 1.0 M urea. ΔG_{H20}° is a measure of protein stability (change in Gibbs free energy between unfolded and native protein states, with no denaturant present, at 25° C and 1M protein concentration), and $\Delta\Delta G_{H20}^{\circ} = \Delta G_{H20}^{\circ}(\text{mut}) - \Delta G_{H20}^{\circ}(\text{wt})$. C_m is the concentration of denaturant at the midpoint of the transition; the larger C_m , the greater the resistance of the protein to denaturation— C_m is a more qualitative measure of protein stability than ΔG_{H20}° . With such a large increase in the free energy of unfolding compared to wt protein, we reasoned that H64F may increase the stability—and therefore yields—of the HGL16 permuted myoglobin. It should be noted that the numbering of amino acid residues is based upon the wt sequence, not the permuted sequence. Data suggest that the folding pathway, folding kinetics, and the MG state of H64F apo-Mb are significantly changed from those of the wt swMb (13). Comparing the stability and structure of H64F-HGL16 to HGL16, H64F-wt swMb, and wt swMb may give us

insights into how point mutations affect topological mutants, and specifically how HGL16 differs from wt in and around the E helix and heme pocket.

The three methods for increasing expression yields of permuted myoglobins will do more than give us more protein; each can tell us—as we characterize the protein produced—about the stability, electrostatic and hydrophobic environments, folding pathway and intermediates, and function of our permuted HGL16.

Materials and Methods

All enzymes were purchased from New England Biolabs (NEB)

Sperm Whale Myoglobin Gene:

The myoglobin gene we are using has been optimized for expression in *E. coli* (15). The synthetic approach which was used to generate the recombinant gene allowed for the incorporation of codons with optimum usage bias, a Shine-Dalgarno sequence and spacer region from the *Pseudomonas putida* cytochrome P-450_{cam} gene to favor high levels of expression, as well as unique restriction sites for future subcloning and mutagenesis experiments (15). The gene was subcloned into the pUC19 expression vector and the recombinant protein was determined to be approximately 10% of the soluble protein in the *E. coli* strain TB-1 (*ara*, Δ (*lac-pro*), *strA*, *thi*, ϕ 80dlacX Δ M15, r-, m+) (15).

Recombinant DNA:

Polymerase Chain Reaction (PCR): All polymerase chain reactions were performed using a Stratagene Robocycler with a hot top. All reactions included 1X Thermopol Buffer (10 mM KCl, 10 mM (NH₄)₂SO₄, 20 mM Tris-HCl pH 8.8 at 25°C, 2

Increasing Expression Yields of Circularly-Permuted Myoglobins

mM MgSO₄, 0.1% Triton X-100 supplied by New England Biolabs), 1 pmol of each primer, 2 mM additional MgSO₄, 1 mM dNTP mixture and 2 units of Deep Vent Polymerase in a total volume of 50 μL. Each cycle consisted of a 30 second melting stage at 95 °C, one minute annealing stage at various annealing temperatures followed by a 30 second elongation stage at 72°C. Each PCR cycled thirty times.

DNA Visualization: DNA was analyzed on 1% w/v agarose gels. Agarose gel electrophoresis was performed for approximately 1.5 hours at 80 V in modified TAE buffer, stained in an ethidium bromide solution (10 mg/mL) for 10 minutes and destained in deionized water for 10 minutes. DNA was visualized on an UV transilluminator, and results were recorded with a Polaroid camera.

DNA Purification: DNA was purified agarose gel using Millipore DNA extraction kits. A small slice of an agarose gel with the desired size DNA was cut from the gel and inserted into the Millipore filter. The filter was spun at 5000 g for 10 minutes to separate the DNA from the agarose. Qiagen kits were also used to purify DNA following the manufacturer's instructions. The Qiagen Minelute system was used to separate large pieces of DNA, such as linear vector, from small fragments less than 100 bp. Qiagen PCR-Prep kits were used to purify small fragments of approximately 500 bp. Qiagen Miniprep kits were used to purify plasmid DNA from *E. coli*.

Restriction Digestions: Digestions were performed in 1X buffer supplied by NEB for the enzyme (or the buffer suggested by NEB for double digestions) at the recommended temperature for two hours. Bovine serum albumin (BSA) was added to reactions as recommended by NEB. The amount of enzyme used per reaction was equal to the number of units in 1μL of undiluted stock.

Ligation: Ligation reactions consisted of 1X ligase buffer (50 mM Tris-HCl, 10 mM MgCl₂, 10 mM DTT, 1 mM ATP, 50 µg/ml BSA, pH 7.8 at 25°C supplied by NEB), approximately 50 to 200ng vector, an equivalent molar amount of insert and 400 units of T4 DNA ligase. Reactions were incubated at 16°C for 16 to 24 hours. The ligase was then heat killed at 65°C for 10 minutes to prepare the reaction for electroporation.

Electroporation: A Biorad Gene Pulser II was used with 1 mm cuvettes, using settings for resistance of 200 ohms, a potential of 1.25 kV/mm, and a capacitance of 25 µF. Approximately 2 to 4 µL of heat killed ligation reaction was added to 100 µL electrocompetent cells (*E.coli* strain XL1-Blue unless otherwise noted). Immediately after the electric discharge, 1 mL of SOC medium (Luria Bertani medium + 200 mM Mg²⁺ and 100 mM glucose) was added to the cuvette. The cells were incubated for one hour at 37°C, then plated on 50 µg/mL ampicillin LB (Luria Bertani medium + agar) agar plates and grown at 37°C overnight.

Construction of the pMAL-HGL16 expression plasmid: HGL16 was PCR amplified from the tanL2 tandem swMb gene construct, using the PCR program mentioned above. The resulting dsDNA fragment was gel-purified, restricted with *Bam*HI and *Pst*I, and ligated into pMAL (NEB). The ligated plasmid was transformed into *E. coli* strain XL1Blue. Transformed cells were grown on LB/ampicillin (50 µg/mL) agar plates overnight, and candidate clones were screened by restriction analysis and a PCR-based clone check with the bottom PCR primer and a pMAL-specific sequencing primer to confirm the presence of the permutein gene. The MBP-HGL16 gene sequence was confirmed by dideoxy sequencing (SAC-25).

Table 1: Maltose-Binding Protein Fusion Primers

MBP-HGL16 PstI primer	MBP-HGL16 BamHI primer
ACGAGAACTGCAGTGATTATGGAT	GAGCGCGGATCCGGTGA CTTCGGTGC
GTCTAGAATGCAGAA	TGACGCTCAG

PCR Clone Check: Colonies were picked from the transformation plates, touched to a gridded plate, and then swirled in 50 uL of doubly-distilled water in 0.5 mL Eppendorf tubes. 50 uL of 1 M NaOH was added, and the cell solution was incubated at 80° C for 10 minutes to lyse the cells. 10 uL of this cell solution was added to the PCR mixture as described above and cycled through the normal run. Primers used include pMAL sequencing primer (for MBP-HGL16) with the HGL16 BamHI bottom primer, or the pTrc99a sequencing primer with the appropriate, opposite HGL16 primer. One other method, useful for plates with only one or two colonies, involves purifying plasmid from overnight cultures of specific colonies. The grid plate with numbered colonies can then be used to make seed stocks if they produce an amplified gene in the PCR.

Creating the H64F-HGL16 gene: Site-directed mutagenesis was performed on an HGL16 template in *pTrc-99a*, using a Quikchange II Mutagenesis kit (Stratagene). The H64F mutation was confirmed by dideoxy sequencing (SAC-45/46). Strain: XL1Blue Gold.

Table 2: H64F-HGL16 mutagenesis primers

HGL16 H64F mutagenic coding primer	HGL16 H64F mutagenic noncoding primer
GAAGATCTGAAAAAATTCGGTGT TACCGTCTTAACTGCC	GGCAGTATTCACGGTAACACCGAATTTT TTCAGATCTTC

Subcloning HGL16 into the pET17b plasmid: Moving HGL16 into pET17b was attempted multiple times but all were unsuccessful. PCR, using pTrc99a-HGL16 as a template, with conditions described above, was successful at amplifying HGL16 gene with the engineered NdeI and KpnI restriction sites; the gene was gel-purified.

Table 3: Primers for moving HGL16 into pET17b

pET17b-HGL16 NdeI primer	pET17b-HGL16 KpnI primer
GGGATTACCATATGGGTGACTTG GGTGTGACGCT	AACGGGTACCCATCATGGATGTCTAGA ATGCAGAACAT

Protein Preparation:

Protein Expression: All permuteins were expressed in 1 L bacterial cultures in 2.8 L Fernbach flasks at 37 °C with shaking of about 200 revolutions/min in a Lab Line Incubator-Shaker. The *E. coli* were grown in LB broth with 50 mg/mL ampicillin until mid log phase ($OD_{600} = 0.5-0.7$) then induced with 0.1 mM isopropylthiogalactoside (IPTG). The cultures were then allowed to grow for an additional 4-5 hours then harvested by centrifugation (4000 g for 10 minutes).

Protein Purification: The harvested cells were resuspended in approximately 30 mL lysis buffer (50 mM Tris-HCl, 17 mM NaCl pH 8.5) then lysed by sonication, using a

Increasing Expression Yields of Circularly-Permuted Myoglobins

Branson Instruments, Inc. Sonifier 450 at power level 6, 50% power. Each sample was allowed to sonicate for 1 minute on, 1 minute off three times or until lysis was complete. The samples were then centrifuged at 21,000 g for 20 minutes and the supernatant retained. The pH of the lysate was adjusted to 8.0-8.5 with 1 M NaOH, and zinc acetate was added to a final concentration of 1 mM. The lysate was centrifuged at 40,000 g for 20 minutes, then filtered through a 0.45 μm filter. Due to the uncommonly high number of surface-exposed histidines in Mb, the filtered lysate was then loaded on a prepared zinc immobilized metal ion affinity column (IMAC) consisting of Amersham Pharmacia Biotech Chelating Sepharose Fast Flow resin. The column was washed with buffer and then the protein was eluted with ethylenediaminetetraacetate (EDTA). The partially purified permutein proteins were concentrated in Amicon Centricon concentrators (YM-10), molecular weight cut off of 10,000 Da, by centrifuging at 5000 g for half hour increments until the total volume was approximately 300 μL (0.5 mM myoglobin). Partially purified wild-type myoglobin was buffer exchanged into 20 mM Tris-HCl pH 8.5 using an Amicon Centriprep-10, molecular weight cut off of 10,000 Da, at 3000 g (4 spins at 30 minutes each). The wild-type myoglobin was then concentrated using a Centricon to approximately 500 μL (1.0 mM myoglobin). After IMAC, permuteins were purified by size-exclusion chromatography using an Amersham Pharmacia Biotech Superdex 75 HR 10/30 size exclusion column (HPSEC) attached to a Varian ProStar high-pressure liquid chromatography (HPLC). The samples were spun at 14,000 g for 15 minutes, then filtered through a 0.2 μm filter. Approximately 500 μL of the prepared protein was then injected on the column. The buffer was 20 mM Tris-HCl, 150 mM NaCl pH 8.0 and was pumped at a rate of 0.5 mL/min. Absorbance at 280 nm was

Increasing Expression Yields of Circularly-Permuted Myoglobins

monitored and fractions were collected corresponding to peaks at this absorbance as well as peaks at A_{409} . The purity of each lot of wild-type myoglobin was assessed using the HPSEC column. All proteins were concentrated again in Centricons to a final concentration of approximately 0.5 mM myoglobin. Protein concentration was determined using $\epsilon_{418} = 128 \text{ mM}^{-1} \cdot \text{cm}^{-1}$ and $\epsilon_{280} = 15.2 \text{ mM}^{-1} \cdot \text{cm}^{-1}$. MBP-HGL16, H64F-HGL16 and apoMb were determined to be more than 95% homogenous by SDS-PAGE and/or analytical reverse phase HPLC.

SDS-PAGE: Proteins were analyzed using sodium dodecyl sulfate polyacrylamide gel electrophoresis (SDS-PAGE). All gels consisted of 10% w/v acrylamide (pH 8.8). Electrophoresis buffer was 25 mM Tris, 250 mM glycine (pH 8.3) and 0.1% w/v SDS. Gel loading buffer used was 50 mM Tris-HCl pH 6.8, 100 mM DTT, 2% w/v SDS, 0.25% w/v bromophenol blue and 10% v/v glycerol. Gels were run for approximately one hour at 50 mA then were stained in Coomassie Brilliant Blue stain (50% v/v methanol, 10% v/v acetic acid, 0.1% w/v Coomassie Brilliant Blue R250) and destained in a 1:3:4 acetic acid:methanol:water mixture. SDS-PAGE gels were stored in a 15% w/v acetic acid solution. Biorad Precision Plus Molecular Weight Standards acted as markers in all gels.

Cleavage of MBP-HGL16. Cleavage studies were performed at 37° C, using chymotrypsin (Sigma) and Genenase (NEB), 100 $\mu\text{g}/\lambda$ at 4 λ , in the SEC buffer in which protein was eluted. Reaction volumes were often 200 λ of 4 $\mu\text{g}/\lambda$ fusion protein + 4 λ of enzyme. Time point samples were analyzed via SDS-PAGE, Western Blot and analytical SEC runs. Western Blots used rabbit antiMb primary antibodies and goat antirabbit

secondary antibodies plus a horseradish peroxidase conjugated developing agent (Biorad).

Apomyoglobin Expression and Purification. pET17b with wt swMb was donated by H. Jane Dyson, and expression followed Dyson lab protocols previously described, with rich medium rather than M9 minimal medium (13). Some changes were made: Inclusion bodies were solubilized using 3M GdnHCl, dialyzed overnight into 20mM Tris pH 7.5, concentrated as above, and purified by HPSEC in 10mM Tris pH 8.5 buffer. SDS-PAGE analysis showed 95% purity. Wt swMb in pET17b was confirmed by dideoxy sequencing (SAC-43/51). Analytical HPLC was performed on a Vydec C4 Reverse-phase column, with a gradient of buffer A (0.1% v/v trifluoroacetic acid in water) to buffer B (80% v/v acetonitrile, 0.1% v/v trifluoroacetic acid) over 30 minutes, starting at 30% B, 70% A and going to 100% B at 30 minutes. ApoMb eluted at 11.9 minutes and holoMb at 12.2 minutes.

Urea Denaturation: All reactions occurred at room temperature (25°C) in 10 mM potassium phosphate, 100 mM KCl buffer pH 8.5. New urea solutions were made for each denaturation, and the concentration of the urea solutions (approximately 10 M) was determined using refractive index¹. A determined amount of buffer, sterile water and 10 M urea were mixed well and met-Mb with oxidized heme was added to a final volume of 400 µL and a final heme concentration of approximately 5 µM. Samples equilibrated overnight. Met-B (oxidized heme) was produced by adding 1.1 molar equivalents of 0.015M potassium ferric cyanide to the stock protein solution. Circular dichroism (CD)

¹ [Urea] (M) = 117.66*ΔN + 29.753*ΔN² + 185.56*ΔN³

spectroscopy at 222 nm and UV-Vis spectroscopy at 409 nm were used to observe the unfolding of protein.

pH Denaturation Studies: pH denaturations were performed as described above for chemical denaturations. Apo-Mb was used in concentrations of ~ 20 μ M. Buffer conditions included a series of 100 mM KHPO₄, KH₂PO₄, glycine and EDTA buffers at pH between 1.85 and 6.0; after diluting buffers 10 fold into the spectral sample, samples were incubated overnight and the pH was checked again before each CD spectrum was taken.

Analysis of Data: Data analysis was carried using Microcal Origin 5.0. Curves describing a two-state transition were fit to the data. In the two-state model, there are no intermediate structures in the unfolding process. The folded myoglobin unfolds to denatured myoglobin and free heme (N \rightarrow D + heme).

Origin was programmed with a non-linear curve fitting function that allowed a dependence of the native and denatured state absorbances on denaturant concentration.

The function is as follows (19):

$$(an+bn*x+((ad+bd*x)*exp(-((bb+mm*x)/RR*TT))))/(exp(-((bb+mm*x)/(RR*TT)))+1)$$

Variables:

an = native state absorbance (A_N)

bn = dependence of native state absorbance on denaturant concentration

ad = denatured state absorbance (A_D)

bd = dependence of denatured state absorbance on denaturant concentration

bb = ΔG^0_{H2O} (kcal/mol)

mm = slope of transition (m) (kcal/(mol*M))

Constants:

RR = 0.0019872 (kcal/(mol*K))

TT = 298.15 (K)

This function calculates best fit curves by optimizing a_n , b_n , a_d and b_d , b_b and m_m . The midpoint of the transition (C_m) was determined by taking the derivative of the curve fit.

Normalization of data for figure 15 involved subtracting the absorbance signal in 8 M urea from each preceding data point, then dividing each data point by the absorbance signal in 0 M urea, to give the fraction folded. $F_n = (A_n - A_{8\text{Murea}}) / A_{0\text{Murea}}$. This equation assumes that the protein is fully folded in native conditions (0 M urea) and fully unfolded in 8 M urea.

Results:

MBP-HGL16 Expression

The fusion protein MBP-HGL16 was expressible, with higher yield and longer post-induction time (PI)—time after addition of IPTG—than observed for direct expression of HGL16. The fusion is maximally expressed at seven hours PI, as verified by Western Blot (data not shown due to poor resolution). The fusion protein was purified from *E. coli* in soluble form as described above; post-IMAC samples are shown in Figure 3 as a check of fusion protein's approximate molecular weight of ~61 kDa. Following purification, MBP-HGL16 yields were calculated at 1.5 mg/L, based upon heme absorbance at 418 nm—this yield was based upon four separate experiments. This yield is five times higher than the current HGL16 yields of 0.3 mg/L (Table 4).

Table 4: Yields of free HGL16 compared to HGL16 fused to MBP, based upon heme absorbance (mg of protein per liter of cell culture).

Free HGL16	MBP-HGL16
0.30 mg/L	1.5 mg/L

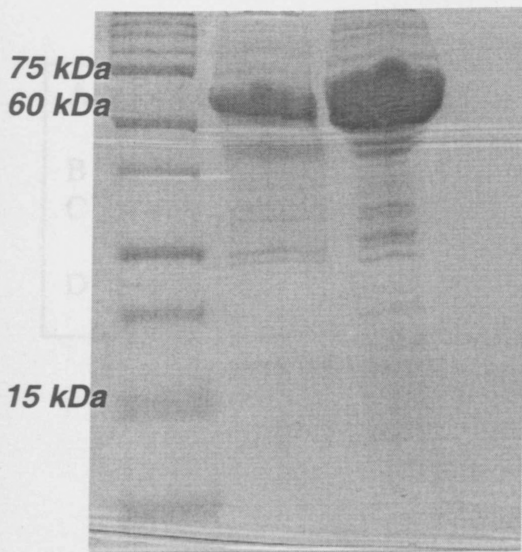
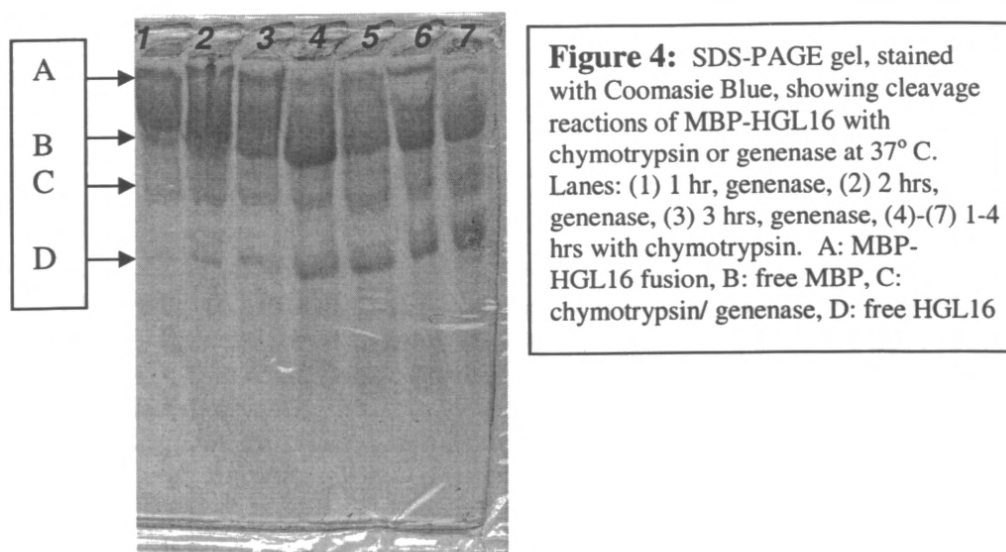


Figure 3: SDS-PAGE showing two representative samples of Coomassie Blue-stained MBP-HGL16 in the right two lanes. Both are post-IMAC purified samples.

MBP-HGL16 Cleavage Optimization

Though the MBP-HGL16 fusion protein can be cleaved with proteolytic enzymes, cleavage proved to be inefficient. NEB designed the pMAL plasmid so that the linker between MBP and the target protein would be specifically cleaved by Genenase, a protease or protein-cleaving enzyme. Genenase did not cleave the fusion protein, while chymotrypsin—a less specific protease—proved able to cleave the fusion protein (Figure 4). Free HGL16 released from the fusion protein made up ~20% of total permuted Mb

present, after cleavage was optimized—from 1.5 mg of HGL16 fusion, 0.30 mg of free HGL16 were liberated. After purification of the products of the cleavage reactions by SEC, too little free HGL16 was collected to make large-scale cleavage/purification more efficient than the direct expression and two column purification of HGL16 procedure already in place.



MBP-HGL16 Denaturation

Urea denaturation of the holo-fusion construct, monitored via absorbance at 409 nm (where the oxidized heme absorbs), shows the HGL16 portion of the fusion to be less stable than free HGL16 (Figure 5a). Curve-fitting analysis using the method of Santoro and Bolen (19) gave $\Delta G^{\circ}_{H20} = 3.5 \pm 1.7$ kcal/mol, $C_m = 3$ M, compared to $\Delta G^{\circ}_{H20} = 7.2$ kcal/mol, $C_m = 4.2$ M for holo HGL16 (Figure 5b). Large errors were generated because few data points constrain the pre- and post-transition baselines. More data, though, require more protein, yet low protein recovery means fewer data points and more error.

This is the very problem we are trying to solve. Without more data in the transitions, these results remain preliminary.

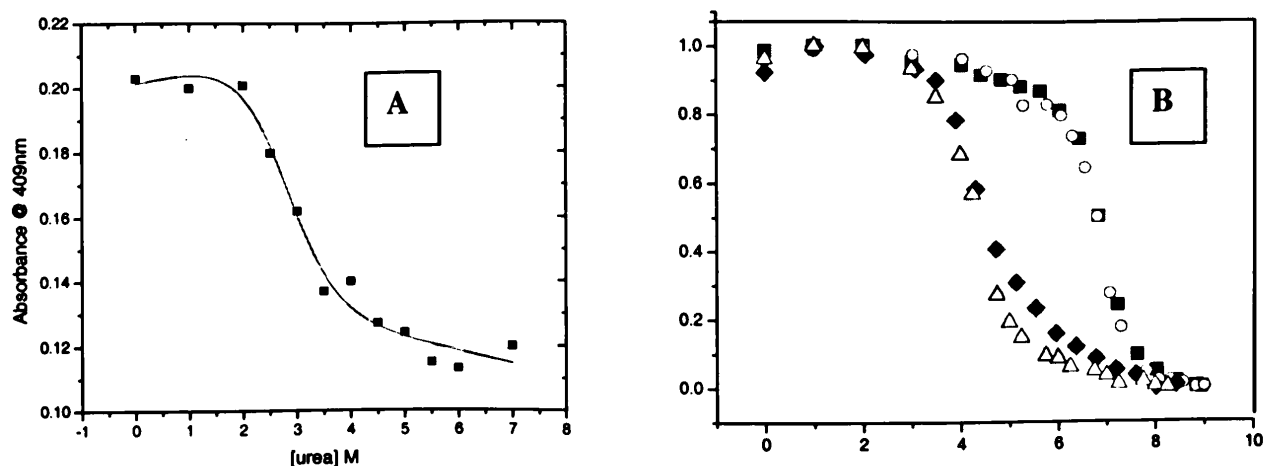


Figure 5: (A) Urea denaturation of MBP-HGL16. Monitored at 409 nm, with calculated curve-fit (19). (10 mM potassium phosphate, 100 mM potassium chloride pH 8.5). Performed at 25° C. (B) Urea denaturation curves of HGL16 (diamonds and triangles) and wt swMb (circles and squares), see ref 3.

Apomyoglobin Purification and Yield

As reported previously (13), expression of wt swMb in the plasmid pET17b yielded large amounts of relatively pure, insoluble inclusion bodies of apoMb. At five hours PI, a large overexpression band corresponding to the MW of Mb was seen in crude cell lysate (lane one, Figure 6); further, a similar band was seen in the soluble cell lysate (lane four, Figure 6), suggesting soluble myoglobin present. After purifying the resobulized, dialyzed inclusion bodies with SEC, >95% purity was achieved for apoMb (Figure 7). The circular dichroism (CD) spectrum of the purified apoMb showed the expected signal characteristic of an alpha-helical protein—minima at 208 and 222 nm (Figure 8). Yields of pure apoMb were much higher than our group historically obtained

using the heme extraction (with methyl ethyl ketone) method (17), which requires holo-Mb as starting material. From 20 mg of holo wt swMb, we would obtain ~5 mgs of purified apo—a recovery of only 25% of sample. Much of the loss is due to protein aggregation. Given past yields of holo wt swMb of 5-6 mg/L, this percentage loss corresponds to 1.25 mg of pure apo—not quite enough for a single denaturation experiment, let alone NMR studies. In the case of permuted myoglobins with low yields, this loss of protein represents a major obstacle to the subsequent characterization of the protein. With the inclusion body purification protocol, yields of pure apoMb approach 20 mg/L (Table 5).

Table 5: Yields of wt apo swMb from holo + heme extraction or direct inclusion body expression (mg of protein per liter of cell culture, as calculated from absorbance at 280 nm).

Holo + heme extraction	Direct expression of apoMb
1.25 mg/L	20 mg/L

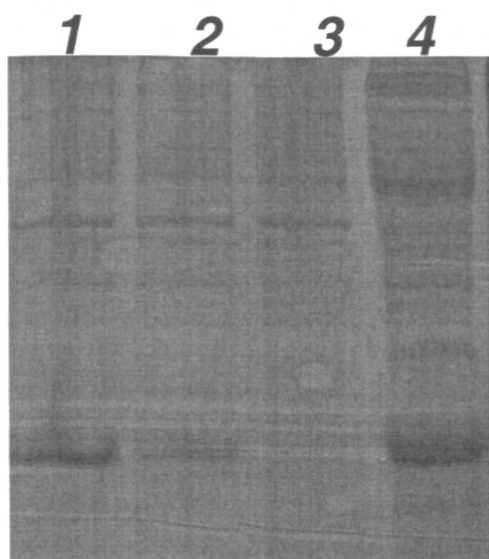


Figure 6: SDS-PAGE gel stained with Coomassie Blue, showing overexpression bands, in crude cell lysate for apoMb expression. Lanes: (1) 5 hours PI, (2) one hour PI, (3) zero hours PI. (4) soluble cell fraction, 5 hrPI

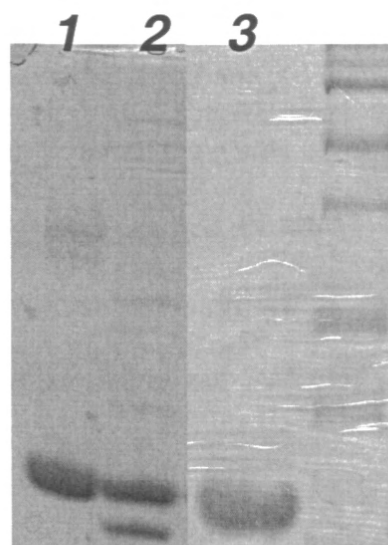


Figure 7: SDS-PAGE gel stained with Coomassie Blue, showing purification of inclusion body apoMb. Lanes: (1) holo wt control, (2) crude inclusion body, (3) SEC- pure apoMb.

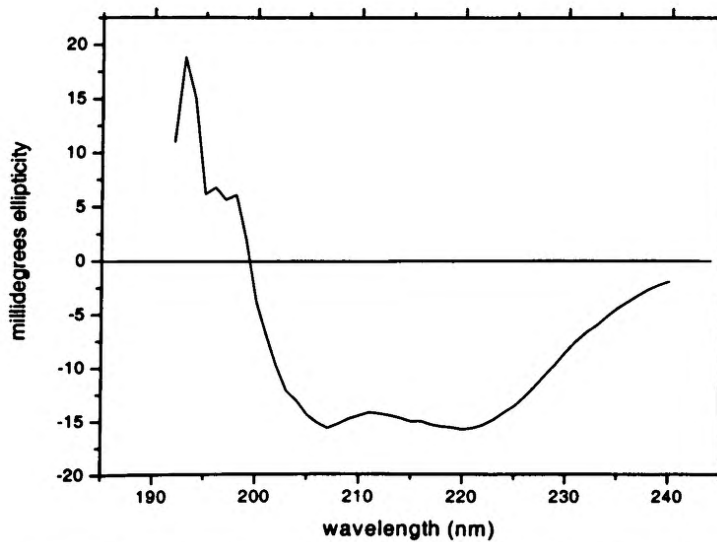


Figure 8: CD spectrum of 20 μ M apoMb (20 mM Tris pH 8.5) purified from inclusion bodies.

HPLC Analysis of Protein Purity

Reverse-phase HPLC experiments show that our apoMb (lane 3, Figure 7) elutes at 37% acetonitrile and comprises >90% of the sample, based upon area under all peaks (91 AU sec for apoMb / 98 AU sec total) (Figure 9a). Our purified apoMb has an elution profile very similar to that of SEC-pure wt holoMb grown and harvested by conventional methods (Figure 9b), yet appears more pure than wt isolated by our 2-column procedure.

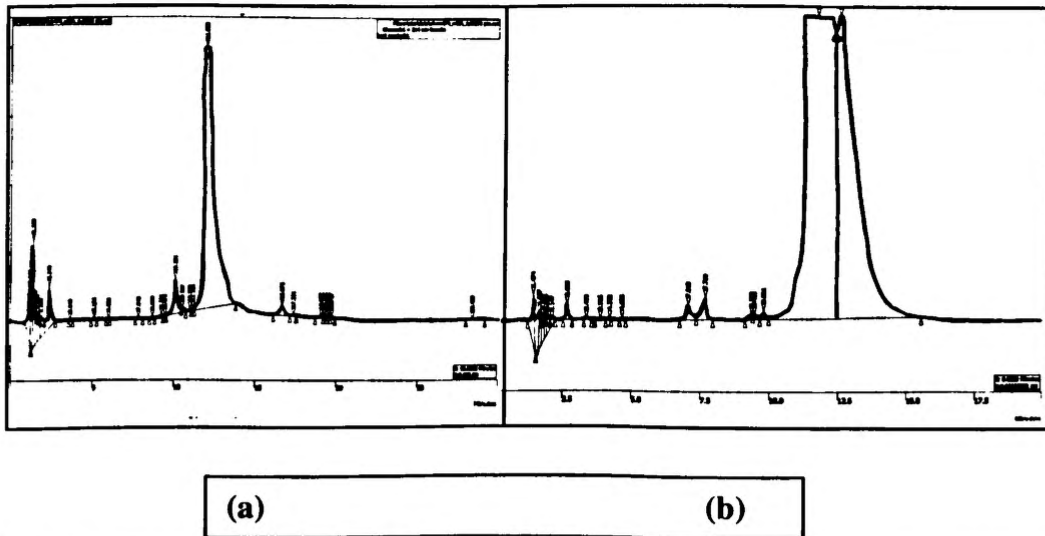


Figure 9: Reverse-phase HPLC chromatogram of directly expressed and purified apoMb (a) versus wt holoMb (b) conventionally expressed and purified. (a) has greater than 90% purity.

Apomyoglobin urea and pH Denaturations

To ensure our purification protocol was sound and useful for future comparisons of apo-HGL16 and apo-H64F-HGL16, we performed both urea and pH denaturations of the apoMb purified from inclusion bodies, monitoring via CD at 222 nm. Our urea denaturation approximated the results of other labs: similar C_{ms} and m -values (13) (Figure 10a). However, our pH denaturations, performed on apoMb confirmed to be pure (Figure 9), produced a large amount of scatter. No intermediate was verified. A representative pH-induced denaturation is shown below (Figure 10b); though a pre-transition baseline is discernible, data at pH near the intermediate are highly scattered, and the post-transition baseline needs more data points to constrain it.

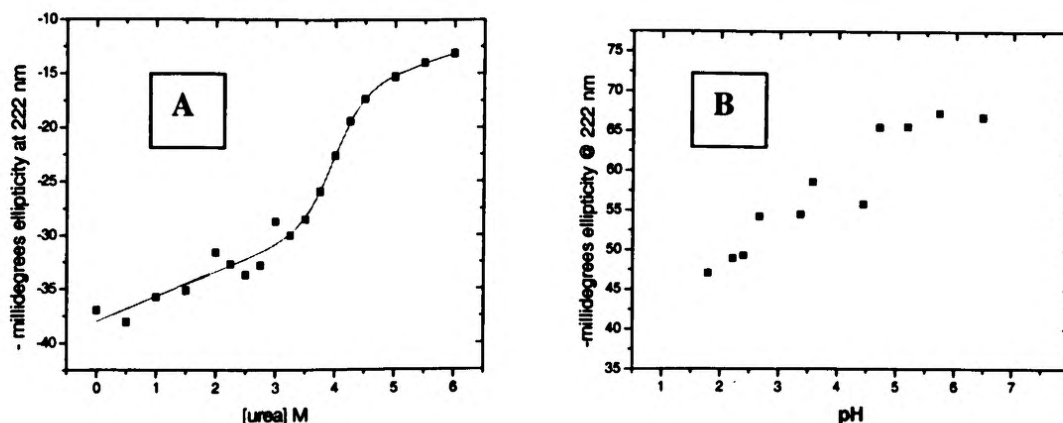


Figure10: CD Urea and pH denaturations of apo wt swMb. **(a)** urea denaturation with calculated curve fit (18) (10 mM K phosphate pH 8.5); **(b)** pH denaturation. Both are monitored at 222 nm. Denaturations were performed at 25 C.

Subcloning HGL16 into pET17b plasmid was unsuccessful

No constructs have been made of HGL16 in pET17b successfully. Double-digests of the pET17b plasmid seemed to be the obstacle: after ligation of doubly-digested gene and vector which has been doubly-digested and gel-purified, colonies that grew after transformation into BL21(DE3) contained only wt swMb as gene insert. Such results suggest that singly-digested plasmid is carried through the gel purification and is religated in the ligation. This may be the result of an enzyme not cutting efficiently or too liberal of cutting when removing bands from agarose gel after double-digestion and gel-purification.

H64F-HGL16 Purification and Preliminary Yields

H64F-HGL16 is expressible from the plasmid pTrc99a; at seven hours post-induction, one liter of cell culture yields red protein after purification, with the characteristic Soret absorbance for the heme at 418 nm. [Seven hours PI was somewhat

arbitrarily defined (and has not been optimized): one liter harvested at four hours PI yielded very little protein, so seven hours PI was used, and more protein was recovered.] Protein was >95% pure after IMAC and SEC purification (Figure 12). A slightly-higher MW contaminant (SEC fraction 1) was separated from pure H64F-HGL16 after SEC (Figures 11 and 12). Preliminary yield, averaged from a six liter purification, was ~ 0.21 mg/L (yields of the HGL16 permuted myoglobin currently average 0.30 mg/L), as calculated from the absorbance of the heme at 418 nm.

However, λ max for the Soret peak shifted from 418 nm to 425 nm (for the reduced form of the heme); further, λ max for the oxidized form of the heme shifted from 409 nm to 395 nm, at pH 7.5 in the absence of denaturant (Figure 13). When 2.0 M urea was added, λ max for oxidized H64F-HGL16 shifted back to 409 from 395 nm. Consequently, denaturation experiments may contain artifacts when monitoring 409 nm on a UV/Vis spectrophotometer. As most previous studies have worked exclusively with directly expressed apo-H64F mutants, changes in λ max and the extinction coefficient have not been published, so, to ensure accuracy in calculating concentrations, absorbance of the tryptophan residues at 280 nm should be used to quantify expression yields of the mutant H64F-HGL16 (Table 6).

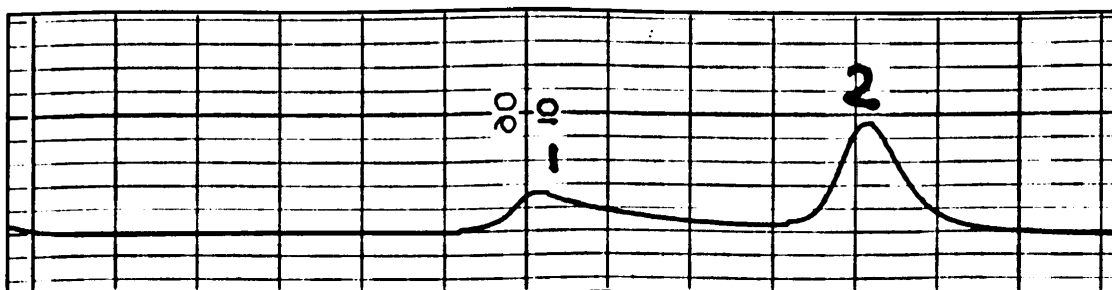


Figure 11: Size-Exclusion Chromatography trace showing the purification of H64F-HGL16, monitored at 418 nm (20 mM Tris pH 8.5).

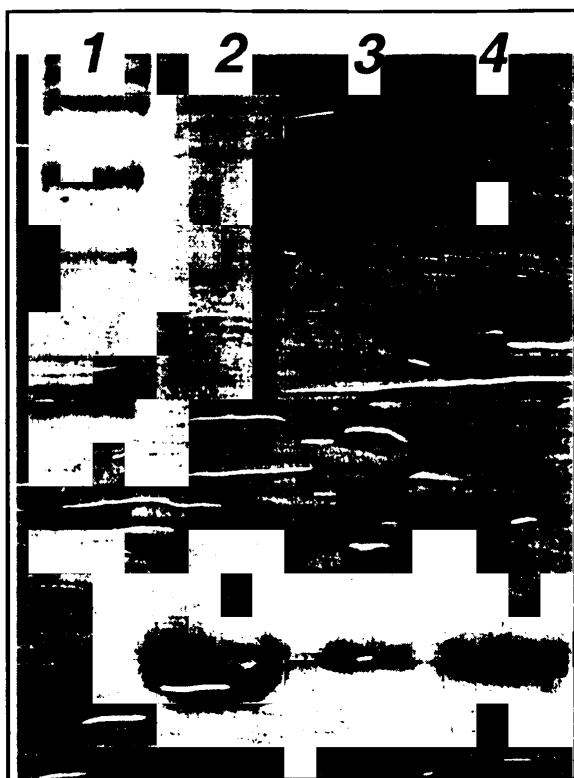


Figure 12: SDS-PAGE gel shows SEC purification of H64F-HGL16. Lane 1: MW Marker, (2) HGL16 control, (3) SEC fraction 1, (4) SEC fraction 2, H64F-HGL16

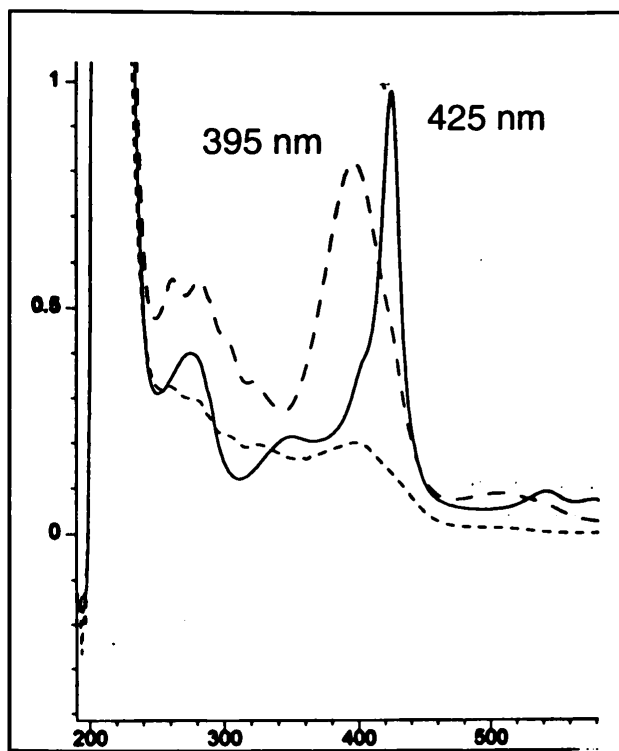


Figure 13: Absorbance traces for H64F-HGL16 with reduced heme (solid line), oxidized (dashed line), oxidized & 4 M GdnHCl (dotted line)

Table 6: Current yield for HGL16 compared to H64F-HGL16 (mg protein/ liter of cell culture) based upon heme absorbance at 418 nm for HGL16 and H64F-HGL16, and tryptophan absorbance at 280 nm for H64F-HGL16.

HGL16 (418)	H64F-HGL16 (418)	H64F-HGL16 (280)
0.30 mg/L	0.21 mg/L	0.37 mg/L

Holo H64F-HGL16 Preliminary Urea Denaturation

Preliminary chemical denaturation of the holo-H64F-HGL16, monitored at 409 nm, was performed to estimate the mutant's stability relative to HGL16. The unfolding curve lacks a pre-transition baseline (Figure 14). Given the observed behavior of λ max in various environments, we might conclude that UV/Vis spectroscopy, monitoring

changes in the heme's absorbance, does not give a true picture of the unfolding of H64F-HGL16 upon addition of chemical denaturants. CD denaturations, monitoring secondary structure rather than the tertiary environment surrounding the heme pocket, should give more reliable information about the urea-induced unfolding of H64F-HGL16.

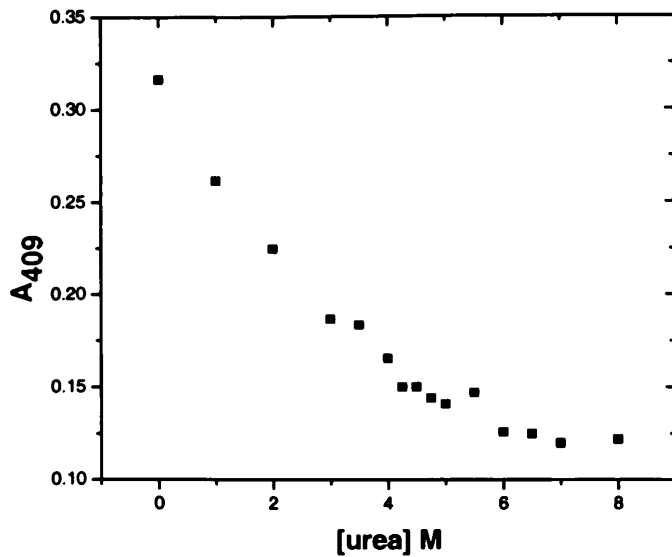


Figure 14: UV/Vis denaturation of 5 μ M H64F-HGL16 lacking a pre-transition baseline. Monitored at 409 nm.

Preliminary CD denaturation and spectrum of H64F-HGL16

As expected, the CD spectrum of H64F-HGL16 shows features of an alpha-helical protein (Figure 15a), with minima at 208 and 222 nm, similar to the CD spectrum of holo HGL16 (Figure 15b).

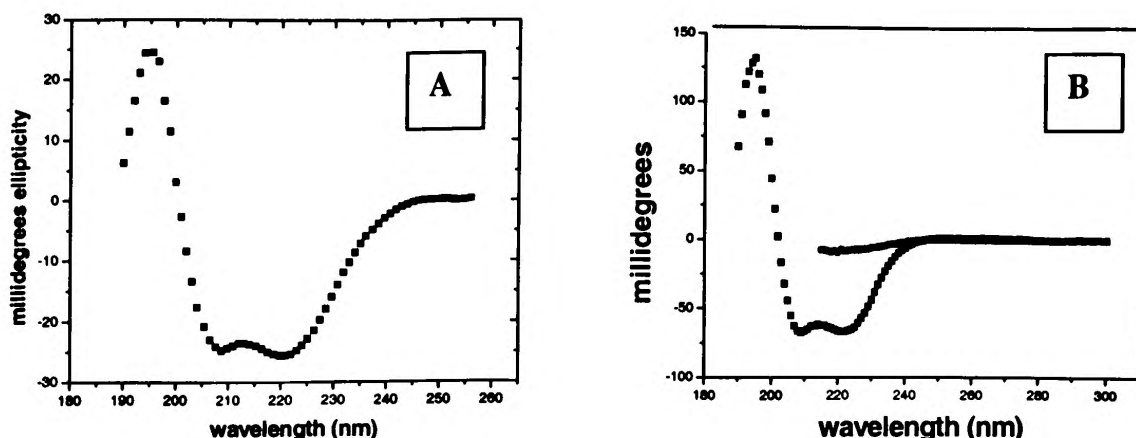


Figure 15: (a) CD spectrum of 6.5 μM holo H64F-HGL16 (10 mM potassium phosphate, 100 mM potassium chloride pH 8.5), (b) CD spectrum of 5 μM holo HGL16 in 0 M and 8 M urea, 100 mM potassium phosphate pH 7.0 (Jennifer (White) Keeffe)

In contrast to wt swMb and wt H64F swMb apo-proteins, the urea denaturation profile of the holo permuted mutant H64F-HGL16, monitored by CD, shows a non-cooperative unfolding transition similar to the UV-Vis-monitored denaturation in Figure 12 (Figure 16a). No pre- or post-transition baseline is seen. This curve is similar to that obtained for apo-HGL16 (Figure 16b). This suggests that the H64F mutation does not exert the same stabilizing effect in the permutein HGL16 that is observed for wt swMb. UV-Vis- and CD-monitored urea denaturation curves for H64F-HGL16 superimpose, suggesting that the UV/Vis data are not artifactual (Figure 17).

Increasing Expression Yields of Circularly-Permuted Myoglobins

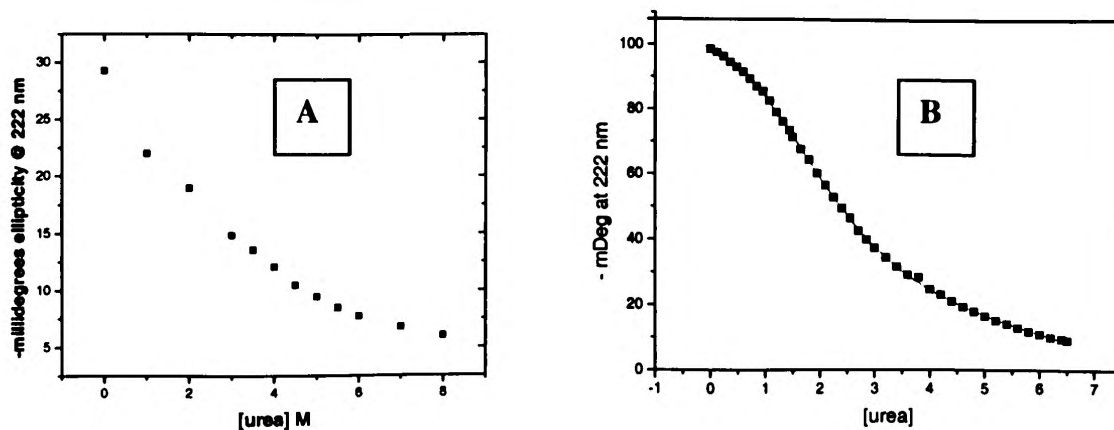


Figure 16: (a) Urea denaturation of 6.5 μ M holo H64F-HGL16 (10 mM potassium phosphate, 100 mM potassium chloride pH 8.5), monitored by CD at 222 nm. (b) denaturation of apoHGL16 with curve fit (18), monitored by CD at 222 nm. Data for (b) collected by Jason Horng, SUNY Stony Brook.

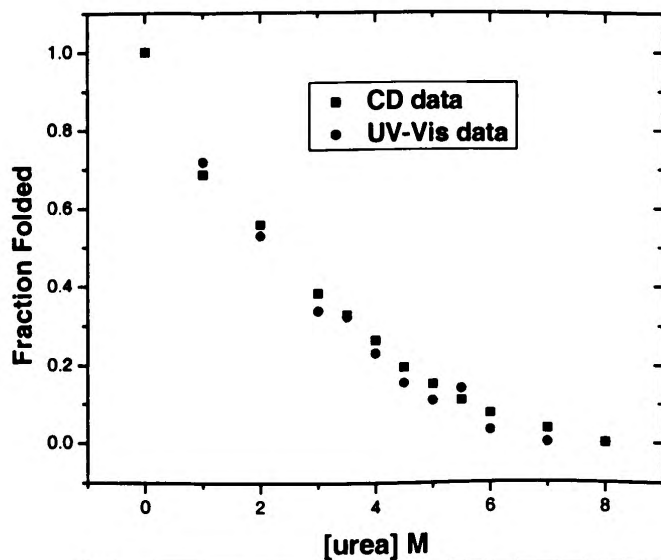


Figure 17: fraction folded, normalized CD- (squares) and UV-Vis-monitored (circles) urea denaturations of holo H64F-HGL16. Data are from Figures 13 and 14 above

Discussion:

Our results show that of the three methods of increasing the yields of permuted Mb, low efficiency in cleavage of MBP-HGL16 makes the fusion system not useful, the inclusion body purification protocol shows much promise, while the H64F mutation in HGL16 may not increase yields but will help us learn how HGL16 compares to wt swMb.

We see that MBP-HGL16 is expressed at higher levels than free HGL16, with yields 5 times higher: 1.5 mg/L vs. 0.30 mg/L (Table 4). Given such a large increase, it would be tempting to think this model system would be at least one potential method for supplying our group with sufficient quantities of easily-purified protein; however, we found that Genenase, which the fusion system is designed to employ (Figure 18), did not cleave the fusion protein.

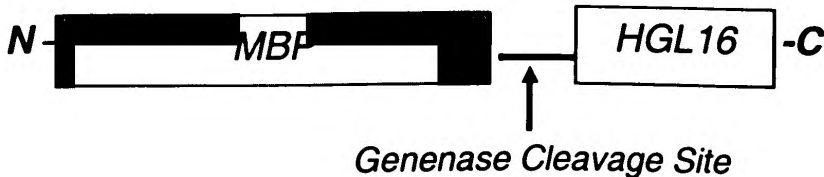


Figure 18: Diagram of MBP-HGL16 fusion protein with Genenase-specific cleavage site.

Little cleavage product was seen at any time point or incubation temperature (Figure 4). Others have had success with chymotrypsin as the protease (Lisa Gentile, personal communication), therefore we experimented with it. Chymotrypsin did cleave the fusion, and after optimizing cleavage, ~20% efficiency was observed; for example, 1.5 mg of HGL16 fusion were incubated and only 300 µg of free HGL16 were recovered. Given that recovery required cleavage at 37° C for two hours and purification with SEC, this

percentage recovery was not sufficient to warrant using MBP fusions as expression systems, because isolated yields of pure HGL16 would be lower than those recovered through direct expression of HGL16. It is possible that HGL16, as with other fusion partners, is fitting snugly into a binding cleft in MBP, protecting it from proteolysis (8). One recent paper reports, however, that denaturing the fusion in guanidine before cleavage results in higher cleavage efficiency (9); thus, higher efficiency in our system might be obtained under denaturing conditions.

Preliminary urea denaturation of the fusion shows that when fused to MBP, HGL16 is destabilized; it may be that fusion to the C-terminus locally destabilizes the H helix. As free MBP has stability comparable to that of holo wt swMb ($C_m \sim 8$ M urea), MBP is not unfolding at the urea concentrations used in experiments shown in Figure 3 (10). So, do we have an example of stability and expression yield not being correlated? Though MBP-HGL16 expresses at higher yields than free HGL16, it is likely that the efficient overexpression and high stability of MBP itself drives the higher level of expression of an apparently destabilized fusion partner HGL16.

Expression of Mb using the T7 promoter of the pET17b plasmid, isolation, resolubilization and dialysis of inclusion bodies, and purification with SEC is an effective way of producing apoMb, with >95% purity. Yields of wt apoMb per liter are up to 20 times higher than those obtained using our previous method of expressing holo Mb and extracting the heme. Further, at eight hours post-induction, 13 mg of holoMb per liter of cell culture are found in the soluble cell lysate (measured by Soret absorbance at 418 nm). Direct expression of apoMb avoids the steps of unfolding, heme extraction, and refolding which account for large losses of protein. Purification schemes based on

inclusion body formation by *E. coli* typically yield very pure protein in relatively few steps.

We have made some modifications to the Dyson protocol (13), and with these modifications, we must ensure that our protein is equivalent to that obtained by the traditional two-column procedure for holo wt, i.e. high enough purity. With our modifications, protein seems equivalent to that obtained by their lab (judging by purity on SDS-PAGE analytical gels, analytical SEC, and urea denaturation). Our reverse-phase HPLC data show good proof that apoMb is >95% pure after purification by SEC, possibly more pure than wt holoMb—although long-term storage of holoMb results in degradation. Realistically, our apoMb is as pure as wt holoMb controls. However, our attempts to replicate other labs' pH denaturations of apoMb were not successful; a great deal of scatter is seen in the data points around the pH intermediate range, though pre- and post-transition baselines are acceptable. This may indicate a difference in the protein sample introduced by the modification of Dyson's protocol, but given our evidence of apoMb purity, the denaturations themselves may simply need to be performed again.

The hope is that direct expression of apo permuted Mbs will allow for extensive characterization of the HGL16 apoprotein. Such characterization would take advantage of the large body of knowledge about apoMb, including stability of various mutants, folding pathways, binding kinetics, and intermediates (3, 11-16). As part of our analysis of how topological mutation affects Mb folding, stability and function, we hope to explore the pH 4.2 intermediate, asking whether HGL16 shows such an intermediate. The presence of the intermediate would indicate similarities in structure and interacting helices compared to wt, and how structured such an intermediate is relative to folded and

unfolded forms of both HGL16 and wt swMb. Once HGL16 is cloned into the pET17b plasmid, work can begin on directly comparing our permutein to wt.

Using absorbance at 280 nm, given the shift in λ max for the heme in H64F-HGL16, we see that expression yields have increased slightly—likely, yields of the permuted mutant are equivalent to yields of pure HGL16. While 0.37 mg of protein lacks luster, such yields are exciting: this is evidence that we can perform site-directed mutagenesis on HGL16, create point mutants, purify them, and compare them to HGL16 and similar wild-type point mutants. While yield may not increase, stability, function or folding pathway may change. We would like to create more point mutants, such as those with altered autooxidation rates (rate at which heme goes from reduced to oxidized), increased CO affinity, to observe how topological mutation affects point mutants known to have specific effects on the function of Mb. We might make an HGL16 double mutant H64Y/V68F to observe changes in heme dissociation rates (20).

H64F, the most stable point mutation in swMb (13), should increase yields of HGL16 dramatically if (a) stability and expression yields are correlated for the permuted globin as they are for the wt Mb (5) and if (b) this mutation increases the stability of HGL16. While we see no evidence for large increases in yield for the permuted mutant, it is not necessarily the case that (a) or (b) above are false. The correlation of stability and expression yield may remain true, as H64F may not change the expression yields because it does not change the stability of HGL16. No change in stability, however, would be quite strange given the precedent in wt and the dramatic change in amino acid character by substitution of Phe for His. His prefers to be solvated, while Phe prefers a hydrophobic environment; as the interior of the heme pocket is relatively hydrophobic,

introducing a Phe in place of His into this region should be entropically and enthalpically favorable. Chemical denaturation studies should illuminate the differences between HGL16 and H64F-HGL16.

With a unique absorbance for both oxidized and reduced heme (395 and 425, versus 409 and 418 nm), H64F-HGL16 has a changed environment near the heme, evidence that the Phe introduction has some effect on the protein. The oxidized form of the heme, with an initial absorbance at 395 nm, shifts back to the typical oxidized heme absorbance at 409 nm upon addition of 2.0 M urea. Such behavior might complicate denaturations monitoring 409 nm; pre-transition baselines may be fouled by the shifting λ max. When urea denaturation of holo permuted mutant H64F-HGL16 is performed and monitored via change in absorbance at 409 nm, no pre-transition baseline is seen; as well, the denaturation curve follows neither sigmoidal nor exponential decay behavior. Curve-fitting proves unreliable, so ΔG°_{H20} cannot be calculated with any confidence. Since the protein is unfolding in the presence of urea, to get a different view of the mutant protein's behavior from that of UV-Vis-monitored changes in heme absorbance, we can monitor changes in secondary structure via CD spectroscopy.

Figure 16a shows another non-sigmoidal, non-cooperative decay protein unfolding as signal and secondary structure diminish. Again, no pre-transition baseline is present, making Santoro and Bolen curve-fitting prone to large errors in determination of ΔG°_{H20} . In fact, these two anomalous curves—which monitor different structural characteristics—are superimposable (Figure 17).

Assuming both curves are either the product of experimental error or some experimental artifact would make interpretation of the data simple: the data are

completely flawed and must be thrown out; however, both curves remain similarly anomalous, rather than singularly so. If we are observing unfolding upon the addition of any amount of denaturant, then perhaps H64F-HGL16 is severely destabilized compared to HGL16, just as apo-HGL16 is destabilized relative to holo-HGL16. Comparing Figure 15 to Figure 14b, we see similar curves for apo-HGL16 and holo-H64F-HGL16; this suggests that the H64F mutation does not exert the same stabilizing effect in the permutein HGL16 that is observed for wt swMb, or perhaps the mutation is stabilizing intermediates relative to the native state.

Our original intention was to transfer the permuted mutant to the pET17b plasmid, in order to express apo-H64F-HGL16, purify it, and characterize it under both urea and pH denaturing conditions. Given our difficulty subcloning HGL16 into the pET17b plasmid, we were unable to get HGL16 in pET17b as the template for our mutagenesis. Attempts to subclone H64F-HGL16 directly into the pET17b plasmid are ongoing.

Conclusions:

Our research has shown, first, that the MBP fusion system, while increasing expression yields of our Mb, destabilizes the fused protein and is not efficiently cleaved. Hence, it is not useful for the purification of HGL16 permuted myoglobins. Second, the direct expression of apoMb and purification of inclusion bodies can be modified for use in our lab. Further, with high yields and one column purification step, it holds much promise for producing enough permuted protein to continue characterizing HGL16, such

as by NMR. Third, mutating permuted HGL16 by substituting Phe for His at residue 64 (115 in HGL16) produces yields similar to wt HGL16. Shifts in heme absorbance and non-cooperative denaturation curves suggest that the mutation does not significantly stabilize the permutein, or stabilizes intermediate states.

In short, increased yields of the permuted myoglobin HGL16 were not realized with all three methods, but they do reveal more about what occurs when a topological mutation is introduced into a well-characterized globin protein such as sperm whale myoglobin: fusing a large protein domain to the H-helix appears to destabilize HGL16, while mutating His64 to Phe affects the heme environment and appears to destabilize HGL16, opposite of its effect on wt swMb. And they raise many more questions: what happens to the structure of the heme pocket when mutations are made in HGL16? How is the folding pathway of swMb affected by the topological mutation HGL16, and how is the folding pathway of HGL16 affected by the wt-stabilizing point mutation H64F? Before rational protein design and engineering can be effective, these questions must be answered.

As Chu *et al.* note, placing point mutations in an engineered protein may populate the native, functional state of a protein relative to a partially-unfolded form, making biotherapeutics more efficacious, biocompatible and stable (21). With our apoMb inclusion body protocol and the H64F and future point mutants of HGL16, we will add more knowledge of engineered protein systems to the collective body, furthering rational drug design and the understanding of how proteins—arguably the most complex biological molecules—fold into functional forms.

References:

1. Shoichet, B. K., Baase, W. A., Kuroki, R., and Matthews, B. W. A relationship between protein stability and protein function, *Proc. Natl. Acad. Sci. U.S.A.* **1995**, *92*, 452-456.
2. Hughson, F.M., Wright, P.E., Baldwin, R.L., Structural Characterization of a partly folded apomyoglobin intermediate. *Science*. **1990**, *249*: 1544-1548.
3. Iwakura, M., Nakamura, T., Yamane, C., Kosuke, M., "Systematic circular permutation of an entire protein reveals essential folding elements," *Nature Struct. Biol.*, **2000**, *7*, 580-585.
4. Fishburn, A. L.; Keefe, J. R.; Lissounov, A. V.; Peyton, D. H.; Anthony-Cahill, S. J.; Circularly Permuted Myoglobin Possesses a Folded Structure and Ligand Binding Similar to Those of the Wild-Type Protein but with a Reduced Thermodynamic Stability. *Biochemistry*. **2002**; *41*(44); 13318-13327.
5. Hargrove, M.S., Kryzwda, S., Wilkinson, A.J., Dou, Y., Ikeda-Saito, M., and Olson, J.S Stability of myoglobin: a model for the folding of heme proteins. *Biochemistry*. **1994**. *33*: 11767-11775.
6. Hammarström, M., Hellgren, N., van den Berg, S., Berglund, H., and Härd T. Rapid screening for improved solubility of small human proteins produced as fusion proteins in *Escherichia coli*. *Prot Sci*. **2002** *11*: 313-321.
7. Shih, Y.P., Kung, W.M., Chen, J.C., Yeh, C.H., Wang, A.H., and Wang, T.F. High-throughput screening of soluble recombinant proteins. *Prot Sci*. **2002**. *11*: 1714-1719.
8. Fox, J. D., Kapust, R.B. and Waugh, D.S. Single amino acid substitutions on the surface of *Escherichia coli* maltose-binding protein can have a profound impact on the solubility of fusion proteins. *Prot Sci*. **2001**. *10*: 622-630.
9. Kapust, R.B. and Waugh, D.S. *Escherichia coli* maltose-binding protein is uncommonly effective at promoting the solubility of polypeptides to which it is fused. *Prot Sci*. **1999**. *8*: 1668-1674.
10. Ganesh,, C., Shah, A.N., Swaminathan, P., Surolia, A., and Varadarajan , R. Thermodynamic Characterization of the Reversible, Two-State Unfolding of Maltose Binding Protein, a Large Two-Domain Protein. *Biochemistry*, **1997**. *36*(16), 5020 -5028.
11. Jamin, M., Yeh, S.R., Rousseau, D.L., Baldwin, R.L. Submillisecond Unfolding Kinetics of Apomyoglobin and its pH 4 Intermediate. *J. Mol. Biol.* **1999**. *292*: 731-740.

12. Loh, S.N., Kay, M.S., Baldwin, R.L. Structure and stability of a second molten globule intermediate in the apomyoglobin folding pathway. *Proc. Natl. Acad. Sci. USA*. **1995**. 92: 5446-5450.
13. Garcia, C., Nishimura, C., Cavagnero, S., Dyson, H.J., and Wright, P.E. Changes in the Apomyoglobin Folding Pathway Caused by Mutation of the Distal Histidine Residue. *Biochemistry*. **2000**. 39(37); 11227 – 11237.
14. Jennings, P.A. & Wright, P.E., Formation of a molten globule intermediate early in the kinetic folding pathway of apomyoglobin. *Science*. **1993**. 262: 892-896.
15. Springer, B. A., and Sligar, S. G. High level expression of sperm whale myoglobin in *Escherichia coli*, *Proc. Natl. Acad. Sci. U.S.A.* **1987**. 84, 8961-8965.
16. BA Springer, KD Egeberg, SG Sligar, RJ Rohlfs, AJ Mathews, and JS Olson Discrimination between oxygen and carbon monoxide and inhibition of autooxidation by myoglobin. Site-directed mutagenesis of the distal histidine *J. Biol. Chem.*, **1989**. 264: 3057 - 3060.
17. Antonini, E., and Brunori, M. (1971) *Hemoglobin and Myoglobin in Their Reactions with Ligands*, Elsevier, North-Holland, New York.
18. Pace, C. N. Determination and analysis of urea and guanidine hydrochloride denaturation curves, *Methods Enzymol.* **1986**. 131, 266-280.
19. Santoro, M. M., and Bolen, D. W. Unfolding free energy changes determined by the linear extrapolation method. 1. Unfolding of phenylmethylsulfonyl α -chymotrypsin using different denaturants, *Biochemistry* **1988**. 27, 8063-8068.
20. Hargrove, M.S., Singleton, E.W., Quillin, M.L., Ortiz, L.A., Phillips, G.N., Jr., Olson, J.S., and Mathews, A.J. His64(E7) Δ Tyr Apomyoglobin as a Reagent for Measuring Rates of Hemin Dissociation. *J. Biol. Chem.*, **1994**. 269, 4207-4214
21. Chu, R., Pei, W., Takei, J., and Yawen Bai. Relationship between the Native-State Hydrogen Exchange and Folding Pathways of a Four-Helix Bundle Protein. *Biochemistry*. **2002**. 41, 7998-9003.